Cluster Compounds

DOI: 10.1002/ange.200463004

Metal Ions Play Different Roles in the Third-Order Nonlinear Optical Properties of d^{10} Metal–Organic Clusters**

Hongwei Hou, Yongli Wei, Yinglin Song, Liwei Mi, Mingsheng Tang, Linke Li, and Yaoting Fan*

Research into nonlinear optical (NLO) materials has become increasingly intensive because of their potential applications in optical fibers, data storage, optical computing, image processing, optical switching, and optical limiting.[1] Thus, the design and synthesis of new materials with large NLO capability represents an active field in modern chemistry, physics, and materials science.[2] Metal clusters are reported to be excellent candidates for NLO materials[3] since they involve dπ–pπ delocalized systems and dπ–dπ conjugated systems.[4] These compounds have a large variety of structures and diverse electronic properties that can be tuned by virtue of the coordinated metal;[5] thus the opportunity exists to tune the NLO properties of metal complexes. Metal clusters can also extend the π-conjugated length, which is one of the many methods used to increase molecular NLO susceptibility $\chi^{(3)}$ values. Moreover, the NLO properties of metal clusters can be enhanced by the introduction of metal→ligand and ligand→metal charge-transfer states.[6] Although many methods can be used to promote the NLO properties of metal clusters, the origination of the NLO properties is the delocalization of the π-electron cloud.[7] This delocalization in metal clusters is mainly brought about by metal ions constructing the skeleton and organic ligands fixing the skeleton, thus both the metal ions and the organic ligands should be important for the nonlinear optical properties of the clusters. To the best of our knowledge, however, all studies confirm that heavy-metal ions play very important roles on the third-order NLO properties of metal clusters because their incorporation introduces more sublevels into the energy hierarchy, which permits more allowed electronic transitions to take place and hence a larger NLO effect to be produced.[8]

[*] Prof. H. W. Hou, Dr. Y. L. Wei, L. W. Mi, Prof. M. S. Tang, L. K. Li, Prof. Y. T. Fan
Department of Chemistry
Zhengzhou University
Henan 450052 (P.R. China)
Fax: (+86) 371-67761744
E-mail: houhongw@zzu.edu.cn
Prof. Y. L. Song
Department of Applied Physics
Harbin Institute of Technology
Heilongjiang 150001 (P.R. China)

[**] This work was supported by the National Natural Science Foundation of China (Nos. 20001006 and 20371042) and the Outstanding Young Foundation of Henan Province.

Supporting information for this article is available on the WWW under http://www.angewandte.org or from the author.

However, we believe that both metal ions and ligands affect the NLO properties from their contribution to the delocalization of the π-electron cloud. If metal ions make a greater contribution than ligands, then the effect of the metal ions on the NLO properties will be greater; however, ligands can also make an important contribution to the NLO properties.

How do we investigate the contribution of metal ions and ligands to the delocalization of the π-electron cloud? The frontier molecular orbital corresponds to the delocalization of the π-electron cloud, so we can understand the contribution of metal ions and ligands to the delocalization of the π-electron cloud by calculating their component of the frontier molecular orbital. We can then deduce whether the metal ions or ligands play more important roles in the NLO properties. This approach has been utilized herein. We prepared 2,6-dicarboxamido-2-pyridylpyridine (H_2dcapp), the unique crownlike cluster $[Ag_{10}(dcapp)_4]\cdot 2(OH)\cdot 12H_2O$ (**1**), as well as clusters $[Zn_4O(dcapp)_3]\cdot 6H_2O$ (**2**) and $[Hg_2(dcapp)_2]$ (**3**), and studied their third-order NLO properties. We determined by quantum chemical calculations the contribution the metal ions and organic ligands make to the NLO properties and found them to be consistent with the experimental results. In addition, we found that the population of the triplet excited state for nanosecond laser radiation is responsible for the third-order nonlinear properties of these compounds.

The reaction of $AgNO_3$ with 0.5 equivalents of H_2dcapp in a mixture of THF, DMF (*N*,*N*-dimethylformamide), and H_2O leads to the formation of the light-yellow decanuclear cluster $[Ag_{10}(dcapp)_4]\cdot 2(OH)\cdot 12H_2O$ (Figure 1).[9] The main unit is a decanuclear silver aggregate $[Ag_{10}(dcapp)_4]^{2+}$, which has a crownlike architecture. The ten silver atoms are arranged in two irregular tetrahedrons (Ag1-Ag1A-Ag2-Ag2A and Ag1B-Ag1C-Ag2B-Ag2C) and a distorted octahedron (Ag2-Ag2A-Ag2B-Ag2C-Ag3-Ag3A). The two tetrahedrons and the octahedron are connected by the two edges Ag2-Ag2A and Ag2B-Ag2C. The edge lengths of the tetrahedra are in the range 2.8329(16)–3.0259(9) Å, and in the octahedron the closest Ag···Ag contacts are found and range from 2.6521(9) to 2.9345(11) Å. The Ag2···Ag3 distance (2.6521(9) Å) is much shorter than that in elemental silver (2.88 Å). The distances of 2.8329(16)–3.0259(9) Å are comparable to 2.88 Å and twice the van der Waals radius for silver atoms (3.44 Å). We could calculate Wiberg bond orders[10] by quantum chemical calculation and found that the Ag2–Ag3 bond order is 0.1354, thus indicating a strong metal–metal bond between the Ag2 and Ag3 atoms, while other Ag–Ag bond orders are in the range from 0.0847 to 0.0371, thus suggesting the existence of further metal–metal bonds. In addition, Wiberg bond orders of Ag–N range from 0.2329 to 0.3453 and the C–C bond orders are about 1.4.

There are three crystallographically distinct silver ions in the decanuclear silver cluster $[Ag_{10}(dcapp)_4]^{2+}$. Ag1 ions are located on both sides of the crown and are coordinated to three nitrogen atoms and three Ag ions; Ag3 ions coordinate with two N atoms and further bond to four Ag2 ions; and Ag2 ions are surrounded by two N atoms and six Ag ions. Each ligand surrounds the silver ions in a helical conformation and functions as a pentadentate building block, in which

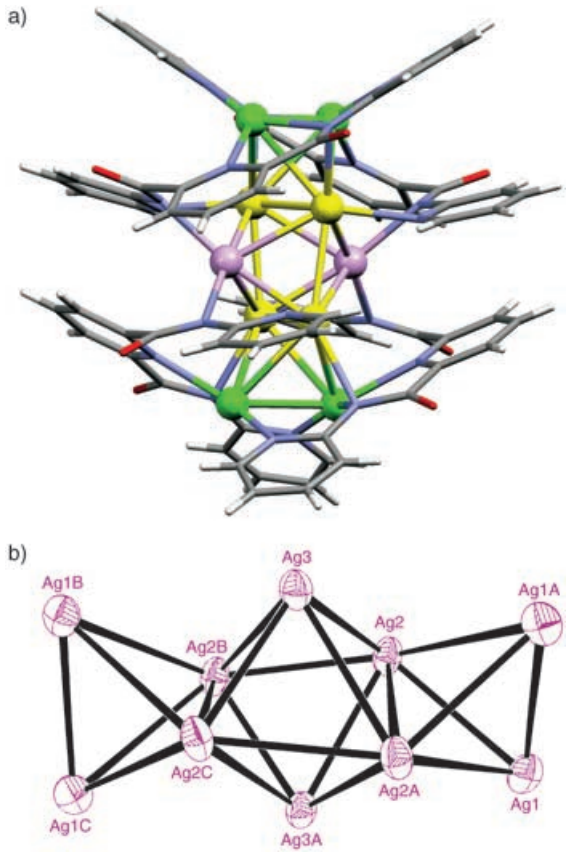

Figure 1. a) Crystal structure of the decanuclear cluster $[Ag_{10}(dcapp)_4]\cdot 2(OH)\cdot 12H_2O$ (**1**). Ag atoms are shown as green, yellow, and pink spheres; O red, N blue, C gray, H white. b) Arrangement of the 10 silver atoms.

N1, N3, N4, and N5 are monocoordinated to a silver center, while N2 acts as a μ_2 donor.

The colorless tetranuclear cluster **2** was prepared from H_2dcapp and $Zn(OAc)_2\cdot 6H_2O$.[9] The arrangement of the zinc ions and the bridging modes of the $dcapp^{2-}$ ligands are shown in Figure 2. The cluster consists of three $dcapp^{2-}$ and four zinc ions and a central oxygen atom. Five N atoms of each ligand coordinate to three Zn ions. The four $Zn–O_{central}$ bond lengths are almost equivalent, and the $Zn\text{-}O_{central}\text{-}Zn$ bond angle (av) is 109.4°. The Zn_4O^{6+} core is an almost perfect tetrahedron, with Zn···Zn separations ranging from 3.117 to 3.240 Å, which is consistent with tetrazinc carbamato complexes having a Zn_4O^{6+} core.[11] Wiberg bond orders of Zn–Zn are about 0.01, thus showing the presence of a weak Zn–Zn metal bond. The corresponding Wiberg bond orders of Zn–O and Zn–N are about 0.38 and 0.26, respectively. The Zn_4O^{6+} cluster ion plays an important role in metal organic frameworks (MOFs), which are novel microporous materials that show potential applications in catalysis, gas storage, and molecular recognition.[12]

The reaction of H_2dcapp with $Hg(OAc)_2\cdot 2H_2O$ leads to colorless block crystals $[Hg_2(dcapp)_2]$ (**3**, Figure 3).[9] The Hg(1)···Hg(2) distance is 3.157 Å, which is comparable to twice the van der Waals radius of Hg atoms (3.10 Å). The Wiberg bond order of Hg(1)–Hg(2) is 0.0106, thus indicating

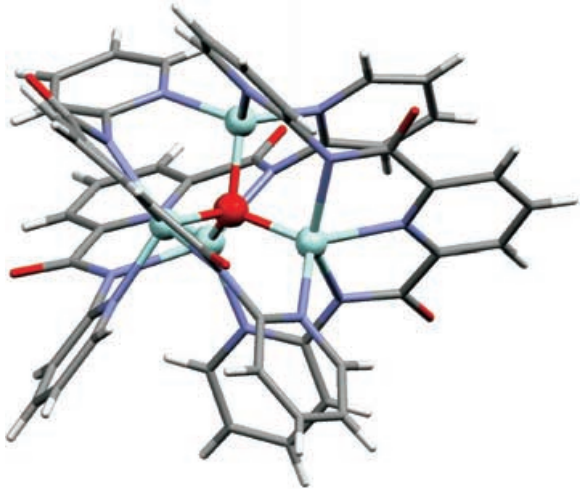

Figure 2. The structure of cluster $[Zn_4O(dcapp)_3]\cdot 6H_2O$ (**2**). Zn pale blue spheres; O red, N blue, C gray, H white.

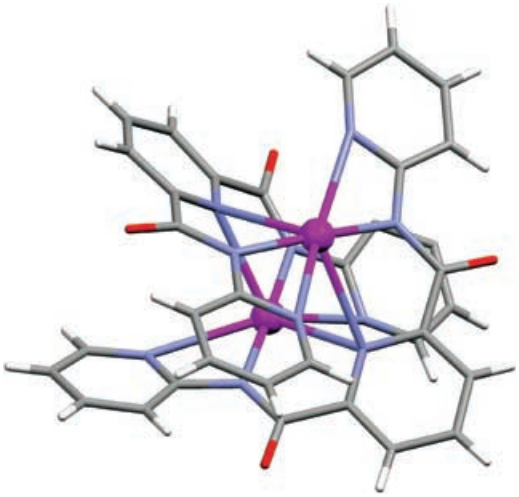

Figure 3. The molecular structure of $[Hg_2(dcapp)_2]$ (**3**). Hg purple spheres; O red, N blue, C gray, H white.

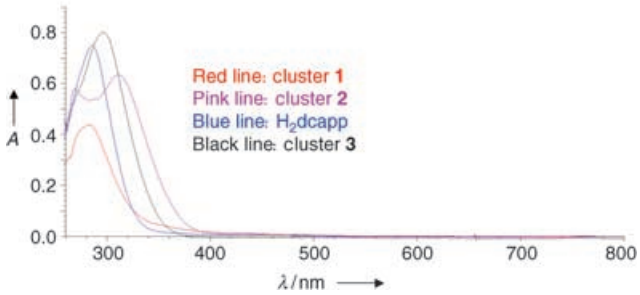

Figure 4. The linear absorption spectra of H_2dcapp, **1**, **2**, and **3**, at 6.2×10^{-4}, 2.0×10^{-5}, 3.7×10^{-5}, and 4.8×10^{-5} M, respectively, in DMF.

wavelength of the laser light (532 nm) is within the nonresonant absorption region.

The NLO absorption components were evaluated by a Z-scan experiment using an open-aperture configuration. Figure 5 depicts the NLO absorptive properties of **1** and

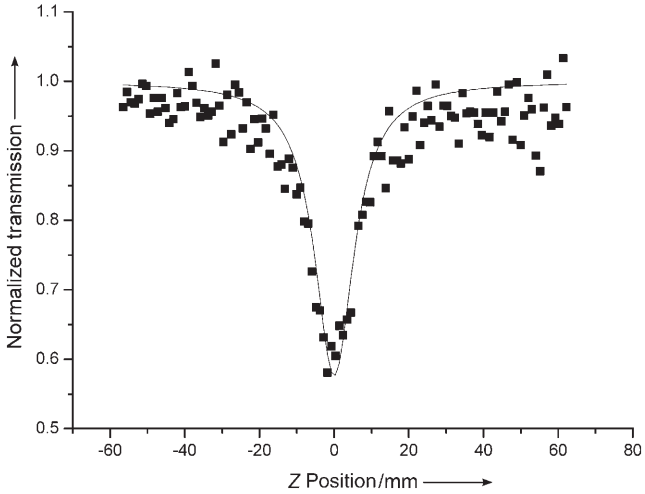

Figure 5. NLO absorptive properties of a 4.1×10^{-4} M solution of $[Ag_{10}(dcapp)_4]\cdot 2(OH)\cdot 12H_2O$ (**1**) in DMF. The black squares are the experimental data, and the solid curve is the theoretical fit.[15]

a weak interaction between the two Hg ions. The corresponding Wiberg bond orders of Hg–N are about 0.52. There are few reports of polynuclear Hg complexes,[13] apart from organomercury compounds.[14] The two $dcapp^{2-}$ ligands wrap helically around the two Hg centers, with the length of the double helix being 3.157 Å.

The third-order NLO properties of **1**–**3** and H_2dcapp were investigated with laser pulses of wavelength 532 nm and duration 8 ns by a Z-scan experiment in DMF solution. The results show that cluster **1** exhibits both very strong NLO absorptive and refractive effects, while H_2dcapp as well as clusters **2** and **3** show weaker NLO absorption and strong NLO refractive behavior. The linear absorption spectra of H_2dcapp and **1**–**3** in DMF are shown in Figure 4. The absorption of the ground state is low in the visible and near-infrared wavelength region (> 380 nm); the maxima of the absorption bands for the ground state are 286 nm for H_2dcapp, 282 nm for **1**, 311 nm for **2**, and 296 nm for **3**. The clearly illustrates that the absorption increases as the intensity of the incident light rises, with light transmittance (T) being a function of the Z position of the samples. A reasonably good fit between the experimental data and the theoretical curves was obtained. This result suggests that the experimentally detected NLO effects have an effective third-order characteristic. It is clear that the theoretical curves qualitatively reproduce the general pattern of the observed experimental data.[16] The nonlinear absorptive index a_2 is calculated to be 1.4×10^{-9} mW^{-1} for a 4.1×10^{-4} M solution in DMF.

The nonlinear refractive components were assessed by dividing the normalized Z-scan data obtained under a closed-aperture configuration by the normalized Z-scan data obtained under the open-aperture configuration. Figure 6 depicts the nonlinear refractive effects of **1**–**3** and H_2dcapp. The valleys and peaks occur at equal distances from the focus. These results are consistent with the notion that the observed optical nonlinearity has an effective third-order dependence

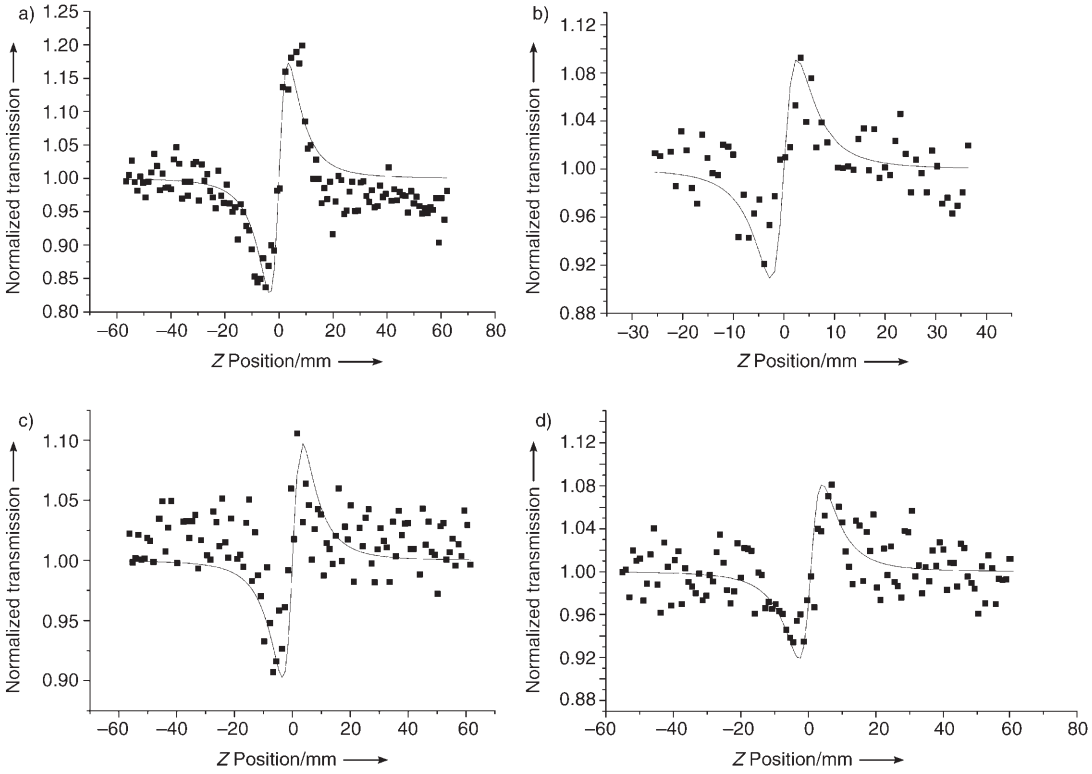

Figure 6. NLO refractive properties: a) $[Ag_{10}(dcapp)_4]\cdot 2(OH)\cdot 12H_2O$ (4.1×10^{-4} M) in DMF; b) $[Zn_4O(dcapp)_3]\cdot 6H_2O$ (7.5×10^{-4} M) in DMF; c) $[Hg_2(dcapp)_2]$ (9.7×10^{-4} M) in DMF; d) H_2dcapp (3.1×10^{-3} M) in DMF. The black squares are the experimental data, and the solid curves are the theoretical fit.

on the incident electromagnetic field.[16] A reasonably good fit between the experimental data (black squares) and the theoretical curves (solid curves) was obtained.[15] The effective third-order refractive index n_2 of **1**–**3** and H_2dcapp are calculated to be 2.2×10^{-11}, 1.2×10^{-11}, 1.3×10^{-11}, and 1.1×10^{-11} esu, respectively.

It is very interesting that the NLO properties of **1** are completely different from those of **2**, **3**, and H_2dcapp. Cluster **1** shows strong NLO absorption and refractive effects, but **2**, **3**, and H_2dcapp only show NLO refractive behavior and give the same refractive index n_2 value. It can be seen from the results that the Ag ions play very important roles in the NLO behavior of **1**, while the influence of the Zn and Hg ions to the optical nonlinearity of **2** and **3** is very small, with the $dcapp^{2-}$ ligands dominating the optical nonlinearity. The reason for this difference cannot be explained by the heavy-atom effect: the strength of the NLO properties can be altered by the π-back-donation capacity of the metal ions to the ligands, and the increased π-back-donation capacity of the metal ions to the ligands may enhance the extension of the electronic π system and improve the NLO properties.[8]

It was reported that the NLO properties of π-conjugated complexes originate from the delocalization of the π-electron cloud.[7] Since the delocalization corresponds to the frontier molecular orbital, we can determine the contribution of the Ag^+, Zn^{2+}, Hg^{2+}, and $dcapp^{2-}$ ions to the NLO properties of clusters **1**–**3** by molecular orbital theory. We have calculated the frontier molecular orbitals of cluster skeletons $[Ag_{10}(dcapp)_4]^{2+}$, $[Zn_4O(dcapp)_3]$, and $[Hg_2(dcapp)_2]$ by density functional theory (DFT) and Hartree–Fock (HF) calculations using the LanL2MB basis set.[17] It can be seen from Figure 7 that the frontier molecular orbitals of $[Ag_{10}(dcapp)_4]^{2+}$, namely HOMO−1, HOMO, LUMO, and LUMO+1, are Ag^+- and $dcapp^{2-}$-based orbitals (DFT/B3LYP 11.08, 5.01, 37.06, 80.84%, respectively, and HF 6.13, 6.94, 63.96, 83.28%, respectively, for Ag^+_{10}): HOMO−1 and HOMO are primarily $dcapp^{2-}$-based orbitals, while LUMO+1 is primarily an Ag^+-based orbital. The frontier molecular orbitals in $[Zn_4O(dcapp)_3]$ (Figure 8) are primarily $dcapp^{2-}$-based orbitals (DFT/B3LYP 0.92, 0.94, 1.80, 2.03%, respectively, and HF 1.48, 1.24, 2.01, 2.22%, respectively, for Zn^{2+}_4), and the four orbitals have barely any Zn^{2+} character. In addition, the frontier molecular orbitals in $[Hg_2(dcapp)_2]$ (Figure 9) are also primarily $dcapp^{2-}$-based orbitals (DFT/B3LYP 1.48, 1.58, 1.58, 1.61%, respectively, and HF 1.88, 1.79, 1.32, 7.50%, respectively, for Hg^{2+}_2). It is usually found that the electron in the highest occupied molecular orbital (HOMO) or the next highest occupied molecular orbital (HOMO−1) is excited to the lowest unoccupied molecular orbital (LUMO) or the next lowest unoccupied molecular orbital (LUMO+1) to give the first excited singlet state S_1 or the first excited triplet state T_1. In general, the photochemical and photophysical properties of compounds are governed by the first excited singlet state S_1 and the first excited triplet state T_1, thus the most important frontier orbital is LUMO or LUMO+1. Both the Ag^+ and $dcapp^{2-}$ ions contribute to the LUMO and LUMO+1 of $[Ag_{10}(dcapp)_4]^{2+}$, while the LUMO and LUMO+1 of $[Zn_4O(dcapp)_3]$ and $[Hg_2(dcapp)_2]$ primarily have $dcapp^{2-}$ charac-

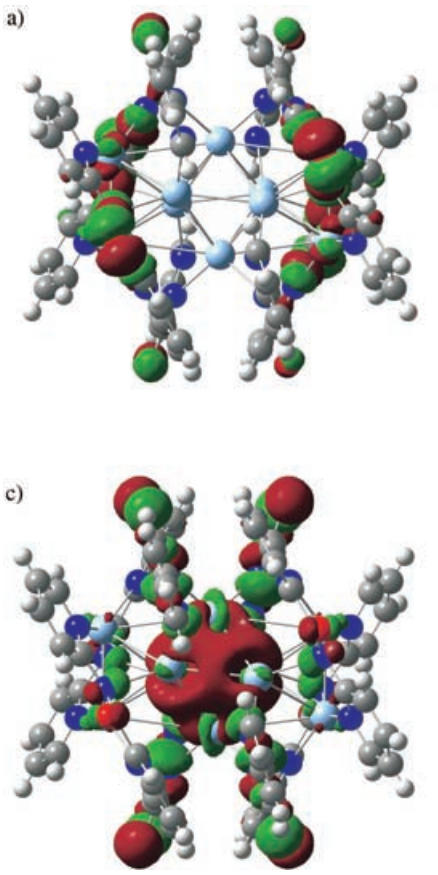

Figure 7. The frontier molecular orbital of $[Ag_{10}(dcapp)_4]^{2+}$: a) HOMO−1, b) HOMO, c) LUMO, d) LUMO+1. Ag light blue, N dark blue, O red, C gray, H white.

ter. Therefore, we can deduce that the NLO properties of cluster **1** are controlled by the Ag^+ and $dcapp^{2-}$ ions while in clusters **2** and **3** the Zn^{2+} and Hg^{2+} ions have no influence on the NLO properties, which are dominated by the $dcapp^{2-}$ ligands. This finding is consistent with the experimental results: **2**, **3**, and H_2dcapp show the same NLO refractive behavior (self-focusing effect) and also have the same refractive index n_2 value, while **1** not only shows a strong NLO refractive effect (self-focusing) but also displays strong NLO absorptive properties. It should be pointed out that both the excited-state population (and absorption) and the two-photon absorption can be responsible for the measured NLO effect.[16] In addition, it can be seen from Figure 7 that there are large dπ–dπ conjugated systems in the LUMO and LUMO+1 of $[Ag_{10}(dcapp)_4]^{2+}$ which can enhance the molecular NLO properties.

The strong nonlinear absorption makes cluster **1** an interesting case for an optical limiting (OL) study. An ideal OL material should be able to respond quickly to the incident light and become increasingly opaque as the incident light increases in intensity. Cluster **1** displays such an OL ability, but **2**, **3**, and H_2dcapp do not; they give weaker OL effects. The optical limiting effect of **1** is depicted in Figure 10. The linear transmittance is 70%. The light energy transmitted starts to deviate from Beer's law as the intensity of the input light reaches 0.03 $J\,cm^{-2}$, and the material becomes increasingly less transparent as the intensity rises. The optical limiting threshold, which is defined as the incident intensity at which the actual transmittance falls to 50% of the corresponding linear transmittance, is 0.15 $J\,cm^{-2}$, with a saturation intensity transmitted of 0.23 $J\,cm^{-2}$. Lower limiting thresholds and saturation levels provide a greater safety margin for device protection. It is interesting to compare cluster **1** with other well-known optical limiting materials for nanosecond pulsed radiation of 532 nm wave-

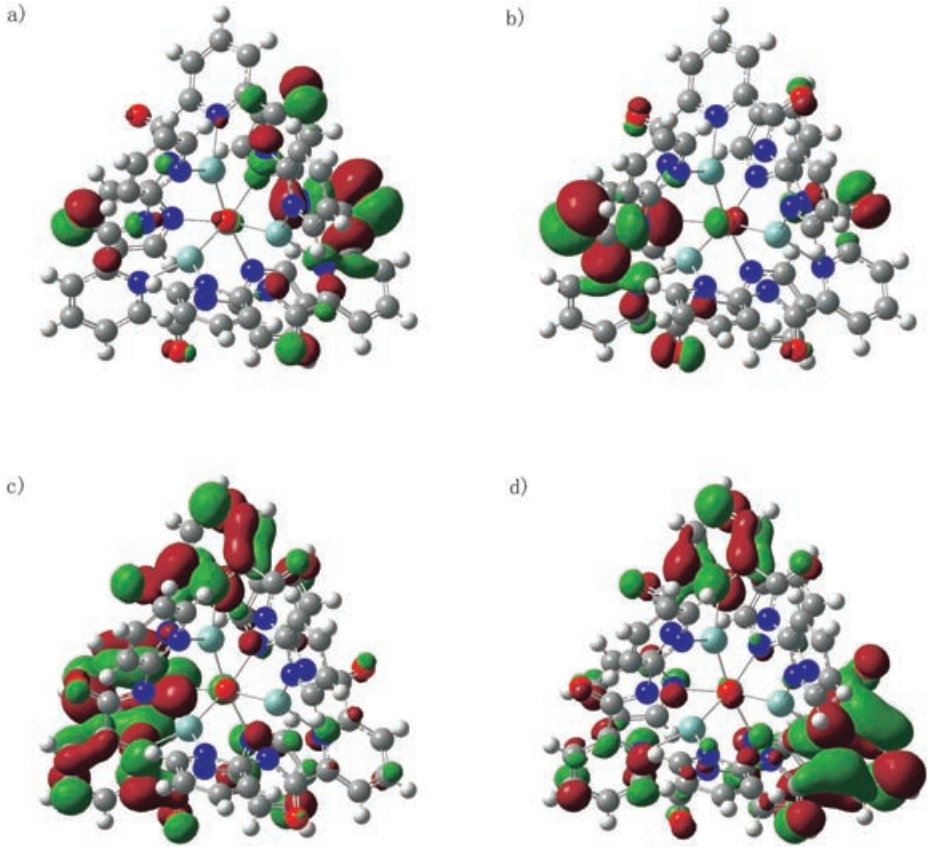

Figure 8. The frontier molecular orbital of $[Zn_4O(dcapp)_3]$: a) HOMO−1, b) HOMO, c) LUMO, d) LUMO+1. Atoms colors as in Figure 2.

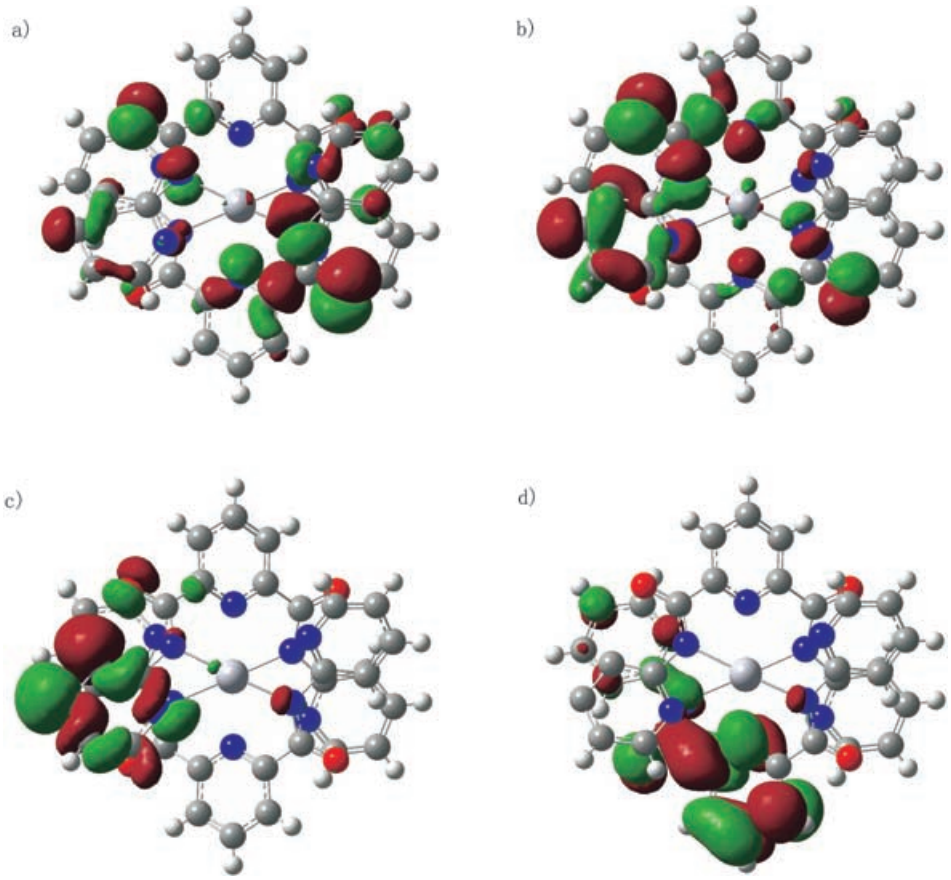

Figure 9. The frontier molecular orbital of $[Hg_2(dcapp)_2]$: a) HOMO−1, b) HOMO, c) LUMO, d) LUMO+1. Hg silver, N blue, O red, C gray, H white.

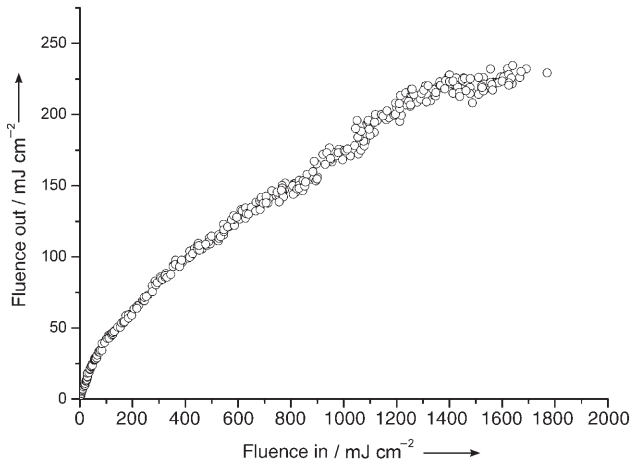

Figure 10. Optical limiting effect of $[Ag_{10}(dcapp)_4]\cdot 2(OH)\cdot 12H_2O$ (4.1×10^{-4} M) in DMF.

length. The optical limiting threshold of **1** (0.15 J cm^{-2}) is lower than that observed in C_{60} and the octanuclear Ag cluster $[Ag_8(2,4,6\text{-}i\text{Pr}_3C_6H_2Se)_8]$.[18] The lower limiting threshold makes cluster **1** a very promising candidate for broadband OL applications.

It should be pointed out that our measurement of the transmitted pulse energy was conducted with a full collection of the transmitted pulse, and no aperture was used. Therefore, the observed OL originates from an NLO absorptive process.[16] Most nanosecond OL performances, such as that of C_{60}, can be interpreted by the five-level (three singlet states and two triplet states) model, and a triplet–triplet transition has been identified as the main mechanism responsible for nanosecond OL effects.[19] Ji et al. developed a five-level model for metal clusters: one ground state, one excited singlet state, one ionized state, one first excited triplet state, and one higher excited triplet state. The initial absorption promotes molecules from the ground to the excited singlet state, the ionized state, and to the first excited triplet state, and then further absorption excites the molecules in the first excited triplet state to the higher excited triplet state. If the absorption cross-section of the triplet state is greater than that of the ground state, then the absorption becomes stronger as the incident intensity increases, which results in an OL effect.[16]

To further study the third-order optical nonlinearity performance of **1**–**3**, and H_2dcapp we investigated their NLO properties with laser pulses of wavelength 532 nm and duration 30 ps by the closed-aperture Z-scan experiment in DMF solution (Figure 11). We find from the data that the closed-aperture Z-scan experimental curves of **1**–**3** and H_2dcapp in DMF solution are the same as that of the DMF solvent for laser radiation of picosecond duration. Moreover, the experimental curve (+) of H_2dcapp at a higher concen-

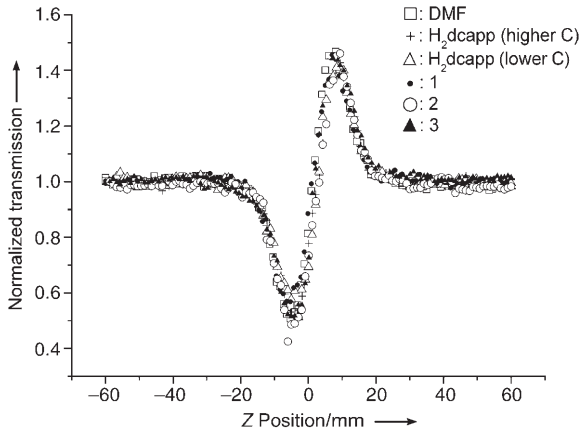

Figure 11. The NLO properties of clusters **1**, **2**, **3**, and H_2dcapp (3.4×10^{-4}, 2.3×10^{-4}, 3.4×10^{-4}, and 2.0×10^{-3} M (or 9.3×10^{-3} M), respectively) in DMF solution, as well as DMF itself, with laser pulses of wavelength 532 nm and duration 30 ps by the closed-aperture Z-scan experiment.

tration (9.3×10^{-3} M) in DMF solution is the same as that (△) of H_2dcapp at lower concentration (2.0×10^{-3} M). Hence, we believe that there exists no third-order optical nonlinearity for **1**–**3** and H_2dcapp with laser radiation of picosecond duration. This result also shows that the population of the singlet excited state cannot contribute to the third-order optical nonlinearity performance of **1**–**3** and H_2dcapp with laser radiation of nanosecond duration. The third-order nonlinearity performance results from the population of the triplet excited state in nanosecond laser radiation. For comparison, the closed-aperture Z-scan experiment of a solution of C_{60} in toluene was also investigated with laser pulses of wavelength 532 nm and 30 ps duration (C_{60} gives strong NLO properties; see Supporting Information). This result illustrates that the NLO performance of C_{60} is brought about by the population of the singlet excited state and triplet excited state in laser radiation of nanosecond duration, and it is different from those of **1**–**3** and H_2dcapp.

Experimental Section

H_2dcapp: 2,6-Pyridyldicarboxylic acid (1.67 g, 10 mmol) was dissolved in $SOCl_2$ (20 mL). The resulting 2,6-pyridinedicarboxylic acid chloride was dissolved in anhydrous pyridine (10 mL), and a solution of 2-aminopyridine (1.90 g, 20 mmol) in pyridine was added dropwise with stirring in an ice bath. Yield: 4.21 g (70%). IR (KBr): $\tilde{\nu}=1698$, 1579, 1545, 1442, 1322, 999, 780 cm^{-1}. Elemental analysis (%) calcd for $C_{17}H_{13}N_5O_2$: C 63.95, H 4.08, N 21.94; found: C 63.14, H 4.51, N 21.81; ^{1}H NMR (400 MHz, DMSO, 25 °C, TMS): $\delta=7.25$ (quin, 2H; C_6H_4), 7.93 (hept, 2H; C_6H_4), 8.31 (hept, 3H; C_6H_3), 8.41 (d, 2H; C_6H_4), 8.50 ppm (d, 2H; C_6H_4); ESI-MS: m/z: 319.9 $[H_2dcapp+H]^+$.

1: The cluster was prepared by reaction of $AgNO_3$ (0.0169 g, 0.1 mmol) with H_2dcapp (0.0161 g, 0.05 mmol) in a mixture of THF (1 mL), water (1 mL), and DMF (4 mL). The reaction mixture crystallized at room temperature on slow evaporation of the solvent to give the desired decanuclear silver cluster as a light-yellow crystalline solid. Yield: 63%. IR (KBr): $\tilde{\nu}=1702$, 1572, 1532, 1439, 1419, 1384, 1319, 1148, 774 cm^{-1}. Elemental analysis (%) calcd for $C_{34}H_{35}Ag_5N_{10}O_{11}$: C 32.15, H 2.75, N 11.03; found: C 33.01, H 2.12, N 11.03.

2: A solution of H_2dcapp (0.0161 g, 0.05 mmol) in DMF (5 mL) was added to a solution of $Zn(OAc)_2\cdot2H_2O$ (0.1 mmol, 0.0219 g) in methanol (5 mL). The mixture solution was left to stand in the air at room temperature for a week, which resulted in colorless crystals suitable for X-ray diffraction analysis. Yield: 46%. IR (KBr): $\tilde{\nu}=$ 1616, 1578, 1556, 1477, 1434, 1381, 1312, 1160, 779 cm^{-1}. Elemental analysis (%) calcd for $C_{51}H_{45}N_{15}O_{13}Zn_4$: C 45.76, H 3.36, N 15.70; found: C 44.98, H 3.21, N 15.38.

3: Complex **3** was prepared in an analogous manner to that used to prepare **2**, except that $Hg(OAc)_2\times2H_2O$ was used instead of $Zn(OAc)_2\times2H_2O$. Yield: 40%. IR (KBr): $\tilde{\nu}=1630$, 1581, 1460, 1433, 1385, 1355, 779 cm^{-1}. Elemental analysis (%) calcd for $C_{34}H_{22}Hg_2N_{10}O_4$: C 39.47, H 2.13, N 13.54; found: C 38.95, H 2.00, N 13.27.

Received: December 21, 2004
Revised: May 31, 2005
Published online: August 11, 2005

Keywords: cluster compounds · density functional calculations · ligand effects · nonlinear optics · silver

[1] a) T. S. Wang, Z. L. Ahmadi, T. C. Green, A. Henglein, M. A. Elsayed, *Science* **1996**, *272*, 1924–1926; b) J. W. Perry, K. Mandour, I. Y. S. Lee, X. L. Wu, P. V. Bedworth, C. T. Chen, D. Ng, S. R. Marder, P. Miles, T Wada, M. Tian, H. Sasabe, *Science* **1996**, *273*, 1533–1536.

[2] a) J. G. Qin, D. Y. Liu, C. Y. Dai, *Coord. Chem. Rev.* **1999**, *188*, 23–34; b) J. L. Bredas, C. Adant. Tackx. *Chem. Rev.* **1994**, *94*, 243–278; c) R. Signorini, M. Zerbetto, M. Meneghetti, R. Bozio, M. Maggini, C. D. Faveri, M. Prato, G. Scorrano, *Chem. Commun.* **1996**, 1891–1892; d) M. Spassova, V. Enchev, *Chem. Phys.* **2004**, *298*, 29–36.

[3] a) S. Vagin, M. Barthel, D. Dini, M. Hanack, *Inorg. Chem.* **2003**, *42*, 2683–2694; b) S. Shi, W. Ji, S. H. Tang, J. P. Lang, X. Q. Xin, *J. Am. Chem. Soc.* **1994**, *116*, 3615–3616; c) W. F. Sun, M. M. Bader, T. Carvalho, *Opt. Commun.* **2003**, *215*, 185–190.

[4] K. Mashima, M Tanaka, Y. Kaneda, A. Fukumoto, H. Mizomoto, K. Tani, H. Nakano, A. Nakamura, T. Sakaguchi, K. Kamada, K. Ohta, *Chem. Lett.* **1997**, 411–412.

[5] a) V. Carcia, P. J. Van Koningsbruggen, H. Kooijman, A. L. Spek, J. G. Haasnoot, O. Kahn, *Eur. J. Inorg. Chem.* **2000**, 307–314; b) A. V. A. Gerard, C. G. Reinier, G. H. Jaap, L. Martin, L. S. Anthony, R. Jan, *Eur. J. Inorg. Chem.* **2000**, 121–126; c) Effendy, F. Marchetti, C. Pettinari, B. W. Skelton, A. H. White, *Inorg. Chem.* **2003**, *42*, 112–117.

[6] a) C. E. Powell, J. P. Morrall, S. A. Ward, M. P. Cifuentes, E. G. Notaras, A. M. Samoc, M. G. Humphrey, *J. Am. Chem. Soc.* **2004**, *126*, 12234–12235; b) N. J. Long, *Angew. Chem.* **1995**, *107*, 37–54; *Angew. Chem. Int. Ed. Engl.* **1995**, *34*, 21–38.

[7] a) T. Wada, L. Wang, H. Okawa, T. Masuda, M. Tabata, M. Wan, M. Kakimoto, Y. Lmai, H. Sasabe, *Mol. Cryst. Liq. Cryst. Sci. Technol. Sect. A* **1997**, *294*, 245–250; b) C. Francis, K. White, G. Boyd, R. Moshrefzadeng. *Chem. Mater.* **1993**, *5*, 506–510; c) S. Morina, T. Yamashita, K. Horie, T. Wada, H. Sadabe, *Rec. Func. Polymer* **2000**, *44*, 183–188; d) H. S. Nalwa, *Adv. Mater.* **1993**, *5*, 341–358.

[8] a) W. B. Lin, Z. Y. Wang, L. Ma, *J. Am. Chem. Soc.* **1999**, *121*, 11249–11250; b) H. W. Hou, X. R. Meng, Y. L. Song, Y. T. Fan, Y. Zhu, H. J. Lu, C. X. Du, W. H. Shao, *Inorg. Chem.* **2002**, *41*, 4068–4075; c) H. Chao, R. H. Li, B. H. Ye, H. Li, X. L. Feng, J. W. Cai, J. Y. Zhou, L. N. Ji, *J. Chem. Soc. Dalton Trans.* **1999**, 3711–3717.

[9] Crystal data for **1**: $C_{34}H_{35}Ag_5N_{10}O_{11}$, $M_r=1299.07$, hexagonal, space group P6(2)22, $a=20.775(3)$, $b=20.775(3)$, $c=17.673(4)$ Å, $\gamma=120°$, $V=6605.8(18)$ Å^3, $Z=6$, $\rho_{calcd}=1.959$ Mg m^{-3}, $\mu=2.249$ mm^{-1}, $F(000)=3792$, $T=291(2)$ K, $\lambda=0.71073$ Å, $R1=0.0452$, $wR2=0.0819$. Crystal data for **2**: $C_{51}H_{45}N_{15}O_{13}Zn_4$, $M_r=1337.50$, triclinic, space group $P\bar{1}$, $a=10.036(2)$, $b=19.327(4)$, $c=19.382(4)$ Å, $\alpha=119.90(3)°$, $V=3259.3(11)$ Å^3, $Z=2$, $\rho_{calcd}=1.363$ mg m^{-3}, $\mu=1.520$ mm^{-1}, $F(000)=1360$, $T=291(2)$ K, $\lambda=0.71073$ Å, $R1=0.0772$, $wR2=0.2033$. Crystal data for **3**: $C_{34}H_{22}Hg_2N_{10}O_4$, $M_r=1033.78$, monoclinic, space group $P2(1)/c$, $a=11.231(2)$, $b=20.994(4)$, $c=13.196(3)$ Å, $\beta=91.34(3)°$, $V=3110.6(11)$ Å^3, $Z=4$, $\rho_{calcd}=2.207$ mg m^{-3}, $\mu=9.918$ mm^{-1}, $F(000)=1944$, $T=291(2)$ K, $\lambda=0.71073$ Å, $R1=0.0677$, $wR2=0.1659$. CCDC 223369–223371 contain the supplementary crystallographic data for this paper. These data can be obtained free of charge from the Cambridge Crystallographic Data Centre via www.ccdc.cam.ac.uk/data_request/cif.

[10] a) K. Wiberg, *Tetrahedron* **1968**, *24*, 1083–1096; b) K. K. Pandey, *Inorg. Chem.* **2003**, *42*, 6764–6767.

[11] C. S. McCowan, T. L. Groy, M. T. Caudle, *Inorg. Chem.* **2002**, *41*, 1120–1127.

[12] a) M. Eddaoudi, J. Kim, N. Rosi, D. Vodak, J. Wachter, M. O'Keeffe, O. M. Yaghi, *Science* **2002**, *295*, 469–472; b) H. L. Li, M. Eddaoudi, M. O'Keeffe, O. M. Yaghi, *Nature* **1999**, *402*, 276–

279; c) O. M. Yaghi, M. O'Keeffe, N. W. Ockwig, H. K. Chae, M. Eddaoudi, J. Kim, *Nature* **2003**, *423*, 705 – 714; d) H. K. Chae, D. Y. S. -Pérez, J. Kim, Y. B. Go, M. Eddaoudi, A. J. Matzger, M. O'Keeffe, O. M. Yaghi, *Nature* **2004**, *427*, 523 – 525; e) M. J. Zaworotko, *Nature* **1999**, *402*, 242 – 243.

[13] C. Brückner, S. J. Retting, D. Dolphin, *Inorg. Chem.* **2000**, *39*, 6100 – 6106.

[14] a) M. Enders, G. Ludwig, H. Pritzkow, *Eur. J. Inorg. Chem.* **2002**, 539 – 542; b) K.-M. Lee, J. C. C. Chen, I. J. B. Lin, *J. Organomet. Chem.* **2001**, *617–618*, 364 – 375.

[15] M. Sheik-Bahae, A. A. Said, T. H. Wei, D. J. Hagan, E. W. Van Stryland, *IEEE J. Quantum Electron* **1990**, *26*, 760 – 764.

[16] W. Ji, H. J. Du, S. Shi, *J. Opt. Soc. Am. B* **1995**, *12*, 876 – 881.

[17] a) C. Lee, W. Yang, R. G. Parr, *Phys. Rev. B* **1988**, *37*, 785 – 789; b) H. B. Schlegel, *J. Comput. Chem.* **1982**, *3*, 214 – 219; c) P. J. Hay, W. R. Wadt, *J. Chem. Phys.* **1985**, *82*, 299 – 310.

[18] a) M. K. M. Low, H. W. Hou, H. G. Zheng, W. T. Wong, G. X. Jin, X. Q. Xin, W. Ji, *Chem. Commun.* **1998**, 505 – 506; b) H. W. Hou, Y. T. Fan, C. X. Du, Y. Zhu, W. L. Wang, X. Q. Xin, M. K. M. Low, W. Ji, H. G. Ang, *Chem. Commun.* **1999**, 647 – 648; c) C. Zhang, Y. L. Song, B. M. Hung, Z. L. Zue, X. Q. Xin, *Chem. Commun.* **2001**, 843 – 844; d) L. W. Tutt, A. Kost, *Nature* **1992**, *356*, 224 – 227; e) C. L. Liu, X. Wang, Q. H. Gong, K. L. Tang, X. L. Jin, J. He, P. Cui, *Adv. Mater.* **2001**, *13*, 1687 – 1690.

[19] a) L. W. Tutt, T. F. Boggess, *Prog. Quantum Electron.* **1993**, *17*, 299 – 338; b) F. Henari, J. Callaghan, H. Stiel, W. Blau, D. J. Cardin, *Chem. Phys. Lett.* **1992**, *199*, 144 – 148; c) D. G. McLean, R. L. Sutherland, M. C. Brant, D. M. Brandelik, P. A. Fleitz, T. Pottenger, *Opt. Lett.* **1993**, *18*, 858 – 860.

